DOI: 10.13208/j.electrochem.180841 **Artical ID**:1006-3471(2018)06-0740-08
Cite this: *J. Electrochem.* **2018**, *24*(6): 740-747 **Http**://electrochem.xmu.edu.cn

Palladium Adatoms on Gold Nanoparticles as Electrocatalysts for Ethanol Electro-Oxidation in Alkaline Solutions

CHEN Hui-mei[1,2,3], ZHU Shang-qian[2], HUANG Jia-le[3], SHAO Min-hua[2*]
(1. *Department of Pharmaceutical Engineering, Zhejiang Pharmaceutical College, Ningbo* 315100, *Zhejiang, P.R. China;* 2. *Department of Chemical and Biological Engineering, The Hong Kong University of Science and Technology, Clear Water Bay, Kowloon, Hong Kong* 999077, *P.R. China;* 3. *Department of Chemical and Biochemical Engineering, College of Chemistry and Chemical Engineering, Xiamen University, Xiamen* 361005, *Fujian, P.R. China.*)

Abstract: Palladium (Pd) is a good catalyst for ethanol electro-oxidation in alkaline solutions. The activity of Pd is further improved in this study by modifying the gold (Au) nanoparticles with Pd adatoms using a simple spontaneous deposition process. The Pd overlayer on the Au core (Au@Pd) is un-uniform with some Au atoms exposed to the electrolyte. The activity of Au@Pd/C toward ethanol oxidation reaction (EOR) is much higher than that of Pd/C in an alkaline solution. The peak current density of Au@Pd/C is 4.6 times higher than that of Pd/C with a 100 mV lower onset potential. The enhanced activity may be due to the electronic effect from the Au core, and the bifunctional reaction mechanism.

Key words: ethanol oxidation; core-shell; electrocatalysis; fuel cells; adatoms
CLC Number: O646; TM911.48 **Document Code**: A

As an alternative power source for portable electronic devices and stationary power plants, direct ethanol fuel cell (DEFC) has attracted significant attention since great achievements have been made[1]. In acidic media, the electro-oxidation of ethanol requires Pt-based electrocatalysts which are very expensive. In alkaline solutions, Pd-based electrocatalysts that are inactive for EOR in acidic media but are quite active at high pH[2-3]. With recent advances in anion-exchange membranes[4-6], alkaline DEFCs have become more promising than before, which inspire more researchers to use non-platinum materials as promising alternative catalysts to study ethanol oxidation reaction (EOR). Great efforts have been devoted to design and synthesize Pd-based bimetallic nanoparticles (NPs) (Pd-Pt[7-8], Au-Pd[9-14], Pd-Ag[15-18], Pd-Ru[19,20], Pd-Ni[21-24], Pd-Sn[25-26], Pd-Co[27-29], Pd-Cu[30], and Pd-Fe[31]). These bimetallic electrocatalysts more or less showed enhanced activities over pure Pd. Among them, Au-Pd bimetallic systems showed great promises[9,32-35]. On an Au-Pd surface, a bifunctional reaction mechanism has been proposed: the catalytic oxidation of CO or CO-like intermediate species was promoted on Au atoms, releasing more Pd active sites[36-37]. Various Au-Pd nanostructures showed 1.4 ~ 3 times of enhancement over Pd NPs in terms of anodic peak current density[12-14,32-34,38]. In a previous study, we synthesized a resembling core-shell structure consisting of an Au core and Pd shell via a Cu underpotential deposition (UPD)-Pd-displacement method[39]. The Pd layer consisting of tiny Pd clusters and pinholes was very active for ethanol oxidation. However, this method involves a complicated Cu UPD process, which is undesirable for large scale synthesis. Herein, we report a simplified protocol only involving the spontaneous deposition of Pd atoms on Au NPs in 2 min. The material synthesized showed comparable activity toward EOR to that fabricated involving Cu UPD.

Received: 2018-08-27, Revised: 2018-09-05 *Corresponding author, Tel: (+852)34692269, E-mail: kemshao@ust.hk

1 Experimental Section

1.1 Preparation of Au/C Nanoparticles

All chemicals were used as-received without any further purification. Carbon-supported Au NPs was prepared according to the literature[40]. Briefly, a vigorously stirred solution of tetraoctylammonium bromide (0.15 g) in 10 mL of toluene was added into 0.031 g of $HAuCl_4 \cdot 3H_2O$ in 5 mL of deionized water. After adding 0.046 g dodecanethiol, the organic phase was isolated and the resulting solution was stirred vigorously for 10 min at room temperature. $NaBH_4$ (0.038 g) in 5 mL of deionized water was then added over a period of 10 min and was further stirred at room temperature for at least another 3 h. After the organic phase was collected, the solvent was removed on a rotary evaporator. The black product was suspended in 10 mL of ethanol, briefly sonicated to ensure complete dispersion. The suspension was filtrated and washed with at least 20 mL of ethanol and 50 mL of acetone. At last, the as-prepared Au NPs were sonicated with carbon in toluene to obtain Au/C sample with a metal loading of ~10%. After the solvent was evaporated, the dried Au/C was heated at 280 °C in a tube furnace in air for 30 min, and then at 400 °C in H_2 for 30 min to remove organic surfactants.

1.2 Surface Modification of Au/C with Pd Adatoms and Electrochemical Evaluation

A uniformly dispersed catalyst ink was prepared by ultrasonic the mixture containing 5 mg of the Au/C, 1 mL of 2-propanol and 20 μL of 5% Nafion (Aldrich) in 4 mL of water for 15 min. A glassy carbon electrode was polished with 0.3 μm alumina powder and cleaned thoroughly. 10 μL of the ink was deposited onto the surface of the glassy carbon electrode and dried under infrared lamp to obtain a thin film. Prior to surface modification, the Au/C-covered glassy carbon electrode was activated between 0.07 and 1.5 V for 10 cycles in an Ar-saturated 0.1 $mol \cdot L^{-1}$ $HClO_4$ (99.999%, Aladdin) solution at a scanning rate of 100 $mV \cdot s^{-1}$. A final cyclic voltammetric (CV) curve was recorded at 50 $mV \cdot s^{-1}$. An Ag/AgCl/KCl (3 $mol \cdot L^{-1}$) leak-free and Pt wire electrodes were used as the reference and counter electrodes, respectively. All the potentials reported in this paper were referred to the reversible hydrogen electrode (RHE). After that, the Au/C electrode was quickly immersed in a 1.0 $mmol \cdot L^{-1}$ Na_2PdCl_4 (99.999%, Alfa Aesar) + 50 $mmol \cdot L^{-1}$ H_2SO_4 (ACS reagent, Sigma-Aldrich) solution to adsorb Pd ions for various time (20, 120, and 300 s, denoted as Au@Pd/C (20 s, 120 s, and 300 s, respectively)). The as-prepared Au@Pd/C electrode was then taken out and rinsed multiple times with deionized water. CV curve of the Au@Pd/C electrode was recorded between 0.07 and 0.8 V for two cycles in an Ar-saturated 0.1 $mol \cdot L^{-1}$ $HClO_4$ solution at a scanning rate of 50 $mV \cdot s^{-1}$. The upper potential limit was set to 0.8 V to minimize the dissolution of Pd[41]. The Cu UPD curves of Au/C and Au@Pd/C electrocatalysts were recorded in an Ar-saturated 50 $mmol \cdot L^{-1}$ H_2SO_4 + 50 $mmol \cdot L^{-1}$ $CuSO_4$ (Reagent grade, Scharlau) solution. The potential range for the Cu UPD was set between 0.33 V and 0.75 V at a scanning rate of 50 $mV \cdot s^{-1}$. The charges associated with Cu UPD were used to estimate electrochemical surface areas (ECAs) of Au/C and Au@Pd/C.

The EOR activity was evaluated by carrying out the electrochemical measurement in an Ar-saturated 1.0 $mol \cdot L^{-1}$ NaOH (ACS reagent, Sigma-Aldrich) + 1.0 $mol \cdot L^{-1}$ ethanol (Gradient grade for liquid chromatography, LiChrosolv) solution in the potential range between 0.07 and 1.2 V at a scanning rate of 50 $mV \cdot s^{-1}$. A Pd/C catalyst (30wt%, TKK) with an average particle size of 3.9 nm (Fig. S1 in the Supporting Information) was used for comparison.

1.3 Nanoparticle Characterization

Transmission electron microscopy (TEM) and scanning transmission electron microscopy with a high angle annular dark field (HAADF-STEM) were employed to characterize nanoparticles on an electron-microscope (Tecnai F30, FEI; Netherlands) with an accelerating voltage of 300 kV.

2 Results and Discussion

A typical TEM image of Au/C is shown in Fig. 1A. The mean particle size is 6.5 ± 1.0 nm by counting about 200 randomly chosen particles from TEM

images. The corresponding histogram of particle size distribution is shown in Fig. 1B. Fig. 2A (black line) shows a typical cyclic voltammogram of the as-prepared 6.5 nm Au/C in an Ar-saturated 0.1 mol·L^{-1} $HClO_4$ solution, which is similar to that of a polycrystalline Au. Prior to the recorded CV curve of Au NPs, Au NPs were cycled for 20 cycles between 0.05 and 1.5 V vs. RHE to clean up the Au surfaces. The Cu UPD curve of the cleaned Au/C sample in an Ar-saturated 50 mmol·L^{-1} $CuSO_4$ + 50 mmol·L^{-1} H_2SO_4 solution at a scanning rate of 50 mV·s^{-1} is shown in Fig. 2B (black line). Two broad current peaks on the anodic and cathodic scans were observed at 0.59 and 0.55 V, respectively. The cathodic peak at 0.55 V was associated with Cu deposition on the Au surface, while the anodic one at 0.59 V corresponded to Cu stripping[42]. Based on the charge associated with the stripping of the Cu monolayer, the ECA of Au/C in Fig. 2B was calculated to be 0.23 cm^2, assuming 420 μC·cm^{-2} for a full Cu monolayer coverage[43-44].

Surface modification of Au surfaces was performed in a 1.0 mmol·L^{-1} Na_2PdCl_4 + 50 mmol·L^{-1} H_2SO_4 solution. The change in the open circuit potential (OCP) of the electrode as a function of time was monitored and the result is shown in Fig. 3. The OCP increased fast in the first 10 s from 0.475 V vs. Ag/AgCl (double layer range of Au/C) to 0.53 V and reached a plateau at ~ 0.54 V in 30 s. The Au/C electrode was kept in the solution for different time (20 s, 120 s, and 300 s) to deposit various amounts of Pd. The CV curve of the as-prepared Au@Pd/C (120 s) electrode is shown in Fig. 2A (red line). A pair of well-defined peaks originated from the adsorption/desorption of H atom was easily distinguished in the potential range of 0.07 ~ 0.4 V. These observed peaks indicated that a Pd overlayer was successfully deposited on Au NPs[45]. On the basis of hydrogen adsorption/desorption region assuming 210 μC·cm^{-2}, ECA of Pd was determined to be 0.11 cm^2, which was lower than the area of Au surface (0.23 cm^2). The lower surface area may be due to the fact that the adsorbed Pd atoms were not fully covered on the whole surface of Au NPs. The Cu UPD curve of Au@Pd/C is different from that of Au/C. One pair of well-defined peaks associated with Cu UPD on Pd was observed at 0.52 (deposition) and 0.54 V (stripping), respectively (red line in Fig. 2B). This observation further demonstrated the existence of a Pd overlayer. In the meantime, a shoulder peak at 0.55 V was also observed on the reverse scan, indicating the incomplete coverage of Pd on Au NPs. This was considered as another evidence for the un-uniform distribution of Pd atoms on Au surface. The surface area derived by the Cu UPD charge (including both Au and Pd atoms) is ~ 0.24 cm^2, which is larger than Pd area from hydrogen adsorption (0.11 cm^2), and Au area from Cu UPD (0.23 cm^2). Based on these values, we can estimate that the Pd coverage is 0.4 ~ 0.5. The Au NP surfaces were not covered with Pd atoms entirely leaving some bare Au atoms exposed to the electrolyte. The similar phenom-

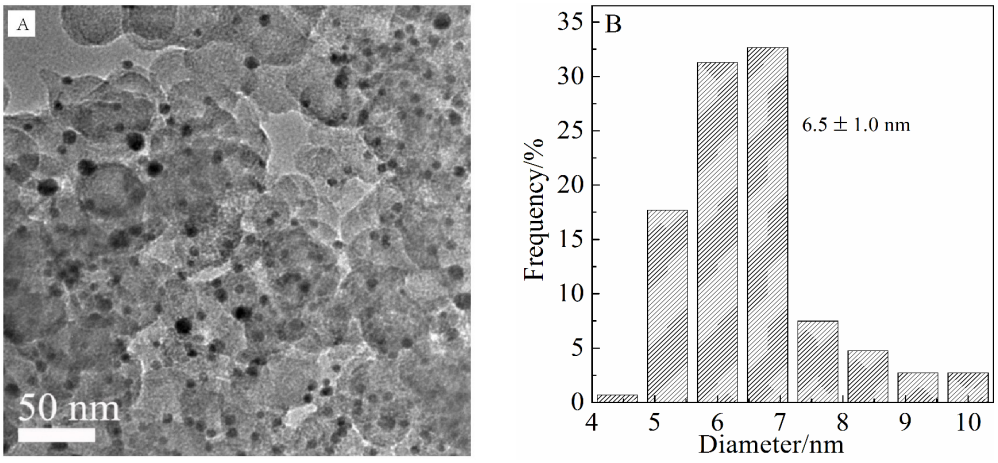

Fig. 1 (A) TEM image of Au/C catalyst and (B) the corresponding histograms of particle size

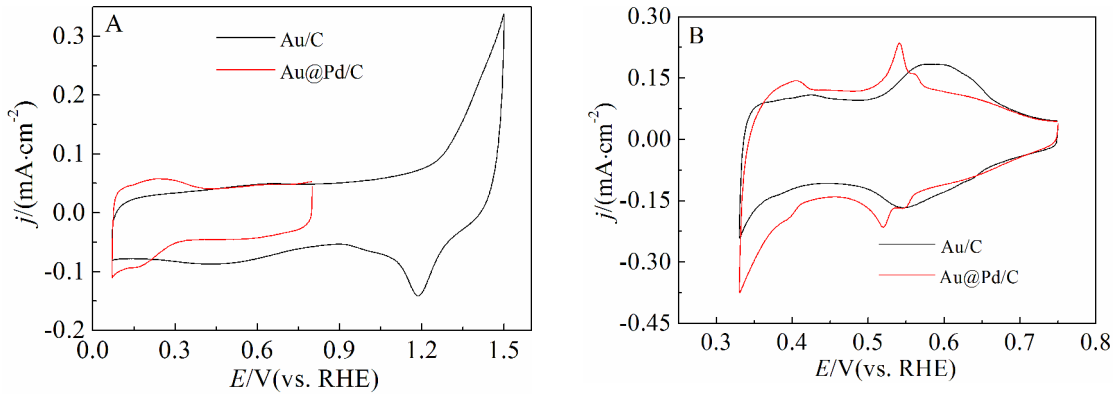

Fig. 2 Cyclic voltammograms of Au/C (black line) and Au@Pd/C (120 s) (red line) electrodes in a deaerated (A) 0.1 mol·L^{-1} $HClO_4$ solution, (B) 0.05 mol·L^{-1} H_2SO_4 + 0.05 mol·L^{-1} $CuSO_4$ solution. Scanning rate = 50 mV·s^{-1}. The currents were normalized to the geometric area of the electrode (0.196 cm^2).

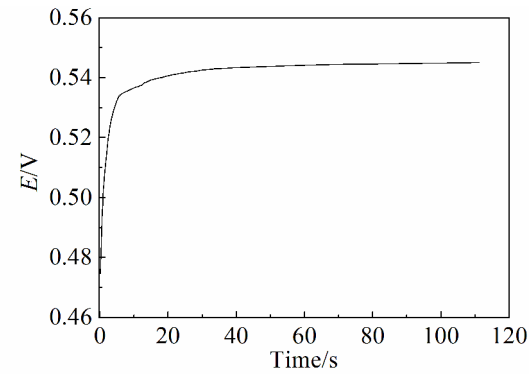

Fig. 3 The open circuit potential as a function of time during the deposition process in 1 mmol·L^{-1} Na_2PdCl_4 + 50 mmol·L^{-1} H_2SO_4 solution. The potentials are referred to the Ag/AgCl electrode.

ena were observed for the samples with different Pd deposition time. Their CVs and Cu UPD curves are compared in Fig. S2.

The as-prepared Au@Pd/C (120 s) NPs were further characterized by TEM, as shown in Fig. S3. It is obvious that Au@Pd uniformly dispersed on carbon black without agglomeration. EDX elemental 2D mapping images (Fig. 4B-D) of an individual Au@Pd (120 s) shown in an HAADF-STEM image (Fig. 4A) were composed of both Au and Pd, suggesting that the latter was successfully loaded on the Au surfaces. Due to the resolution limitation, this technique, however, cannot distinguish well between a core-shell structure and a bimetallic alloy, or reveal the un-uniformity of the Pd shell. Similar elemental mapping results were obtained for both Au@Pd/C (20 s) and Au@Pd/C (300 s) NPs in Fig. S4 and S5.

The electrocatalytic activities for EOR of Au@Pd/C catalysts were evaluated by measuring the voltammograms in an Ar-saturated 1.0 mol·L^{-1} NaOH + 1.0 mol·L^{-1} ethanol solution, as shown in Fig. 5A. Their CV curves were stabilized after about 25 potential cycles. For comparison, the activity of Pd/C (3.9 nm) was also recorded. All the current densities were normalized with respect to the ECAs derived from Cu UPD. The EOR curves on both Au@Pd/C and Pd/C were characterized by two well-defined current peaks on the forward (positive) and reverse (negative) scans, respectively. In the for-

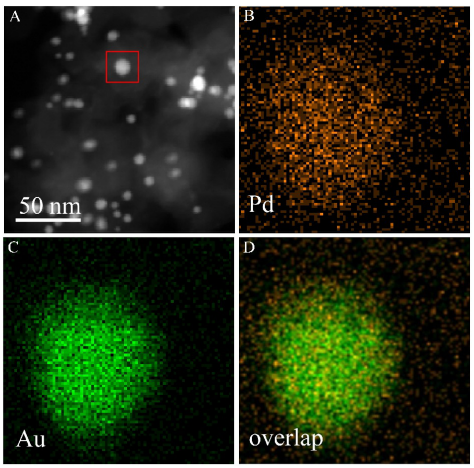

Fig. 4 (A) An HAADF-STEM image of the as-prepared Au@Pd (120 s) NPs, (B-D) EDX elemental 2D mapping images of Pd (orange), Au (green), and overlap.

ward scan, the oxidation peak was ascribed to the oxidation of freshly chemisorbed ethanol[7, 46]. At more positive potentials, the dropping of oxidation current was attributed to the Pd oxidation and less active sites[2]. In the negative scan, the current peak was primarily associated with removal of carbonaceous species which were not completely oxidized in the forward scan, and consequent oxidation of freshly adsorbed ethanol[2, 7, 46].

In the positive scan, the oxidation of ethanol started at about 0.41 V for Au@Pd/C (120 s) electrode, which was ~100 mV more negative than that on Pd/C. The similar potential shift was also observed for the current peak (0.82 V for Au@Pd/C vs 0.9 V for Pd/C) in the positive scan. The negative shifts of the onset and peak potentials indicated that Au@Pd/C catalysts can enhance the electro-oxidation kinetics of ethanol. The onset and current peak potentials for the three Au@Pd/C electrocatalysts with different immersing time in Pd solution were similar, while the peak current densities were greatly different. The electrocatalytic performance in terms of peak current density followed the order Au@Pd/C (120 s) > Au@Pd/C (300 s) > Au@Pd/C (20 s) > Pd/C. The peak current density of Au@Pd/C (120 s) was 30.8 mA·cm^{-2}, which was about 1.6, 1.9 and 4.6 times than that of Au@Pd/C (300 s) (19.7 mA·cm^{-2}), Au@Pd/C (20 s) (16.1 mA·cm^{-2}) and commercial Pd/C (6.7 mA·cm^{-2}), respectively. When the surface modification time is too short, most Pd atoms are in the single atom form, which is not very active for EOR as this reaction requires two neighboring atoms for ethanol adsorption[47]. On the other hand, large Pd clusters are formed when the time is too long. It is worth noting that the performance of Au@Pd/C (120 s) is compatible to that of Au@Pd made of Pd displacement of Cu UPD layer (36 mA·cm^{-2})[39]. In our previous work, we proposed that the ligand effect and lattice mismatch between the Au core and Pd overlayers, and bifunctional mechanism could be responsible for the improved EOR activity of Au@Pd[39].

The long-term performance of the Au@Pd/C (120 s) was assessed by recording the current with time at 0.7 V in an Ar-saturated 1.0 mol·L^{-1} NaOH + 1.0 mol·L^{-1} ethanol solution. As shown in Fig. 5B, both Au@Pd/C and Pd/C show an obvious initial current decay followed by a slower attenuation before reaching the quasi-steady state. The decrease of current is mainly caused by the mass transfer of the reactants and the gradually built-up CO_{ad} on Pd surfaces. The initial current density decay of Pd/C was faster than that of Au@Pd/C (120 s). This implies that the latter owns a higher tolerance to the poisoning of the adsorbed species.

3 Conclusions

The Au NPs modified by Pd atoms with a simple

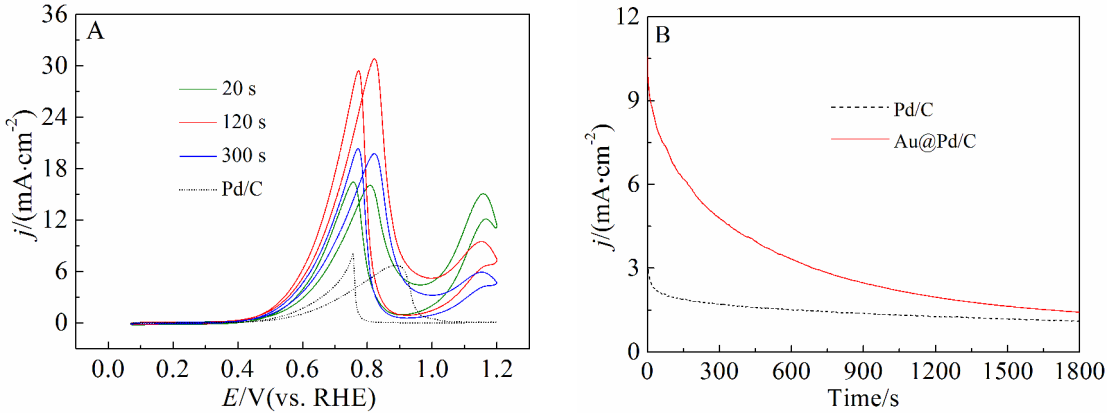

Fig. 5 (A) Cyclic voltammograms of ethanol electro-oxidation for Pd/C (3.9 nm) and Au@Pd/C (20 s, 120 s and 300 s), (B) Current-time curves of ethanol electro-oxidation at 0.7 V for Pd/C and Au@Pd/C (120 s) electrocatalysts in an Ar-saturated 1.0 mol·L^{-1} NaOH + 1.0 mol·L^{-1} ethanol solution at a scanning rate of 50 mV·s^{-1}. The currents were normalized to the corresponding ECAs.

spontaneous process showed excellent activities for ethanol oxidation in alkaline solutions. The onset potential of EOR on the modified Au surface was reduced by ~ 100 mV compared with Pd. More importantly, the peak current density was also increased by 4.6 times. The activity enhancement might origin from the electronic and strain effects from the Au core, and the bifunctional catalytic mechanism in the Au-Pd system. The simple synthesis procedure and excellent activity make Au@Pd a promising electrocatalyst for ethanol electro-oxidation.

Acknowledgements

The authors would like to acknowledge the support from Research Grant Council (No. 26206115) of the Hong Kong Special Administrative Region and Scientific Research Fund of Zhejiang Provincial Education Department (No. Y201840545). Hui-mei Chen would like to thank the scholarship from Xiamen University and The Hong Kong University of Science and Technology. Shang-qian Zhu thanks HKJEBN Group for providing the Ph.D. scholarship.

Supporting Information Available

The supporting information is available free of charge via the internet at http://electrochem.xmu.edu.cn.

References:

[1] Kamarudin M, Kamarudin S, Masdar M, et al. Review: Direct ethanol fuel cells[J]. International Journal of Hydrogen Energy, 2013, 38(22): 9438-9453.

[2] He Q, Chen W, Mukerjee S, et al. Carbon-supported PdM (M=Au and Sn) nanocatalysts for the electrooxidation of ethanol in high pH media[J]. Journal of Power Sources, 2009, 187(2): 298-304.

[3] Ma L, Chu D, Chen R R. Comparison of ethanol electro-oxidation on Pt/C and Pd/C catalysts in alkaline media[J]. International Journal of Hydrogen Energy, 2012, 37(15): 11185-11194.

[4] Dekel D R. Review of cell performance in anion exchange membrane fuel cells[J]. Journal of Power Sources, 2018, 375: 158-169.

[5] Wang Y, Wang G W, Li G W, et al. Pt-Ru catalyzed hydrogen oxidation in alkaline media: Oxophilic effect or electronic effect? [J]. Energy & Environmental Science, 2015, 8(1): 177-181.

[6] Varcoe J R, Atanassov P, Dekel D R, et al. Anion-exchange membranes in electrochemical energy systems[J]. Energy & Environmental Science, 2014, 7(10): 3135-3191.

[7] Chen X M, Cai Z X, Chen X, et al. Green synthesis of graphene-PtPd alloy nanoparticles with high electrocatalytic performance for ethanol oxidation[J]. Journal of Materials Chemistry A, 2014, 2(2): 315-320.

[8] Lin Y F, Tian N, Xiao C, et al. Effects of atom arrangement and thickness of Pt atomic layers on Pd nanocrystals for electrocatalysis[J]. Electrochimica Acta, 2018, 271: 519-525.

[9] Wang W J, Zhang J, Yang S C, et al. Au@Pd core-Shell nanobricks with concave structures and their catalysis of ethanol oxidation[J]. ChemSusChem, 2013, 6(10): 1945-1951.

[10] Li T Q, Zhou H H, Huang J Q, et al. Facile preparation of Pd-Au bimetallic nanoparticles via *in-situ* self-assembly in reverse microemulsion and their electrocatalytic properties[J]. Colloids and Surfaces A: Physicochemical and Engineering Aspects, 2014, 463: 55-62.

[11] Cherevko S, Xing X, Chung C H. Pt and Pd decorated Au nanowires: Extremely high activity of ethanol oxidation in alkaline media[J]. Electrochimica Acta, 2011, 56(16): 5771-5775.

[12] Sebastián V, Zaborenko N, Lei G, et al. Microfluidic assisted synthesis of hybrid Au-Pd dumbbell-like nanostructures: Sequential addition of reagents and ultrasonic radiation[J]. Crystal Growth & Design, 2017, 17(5): 2700-2710.

[13] Shen S Y, Guo Y G, Luo L X, et al. Comprehensive analysis on the highly active and stable PdAu/C electrocatalyst for ethanol oxidation reaction in alkaline media[J]. Journal of Physical Chemistry C, 2018, 122(3): 1604-1611.

[14] Zhang G R, Wu J, Xu B Q. Syntheses of sub-30 nm Au@Pd concave nanocubes and Pt-on-(Au@Pd) trimetallic nanostructures as highly efficient catalysts for ethanol oxidation[J]. Journal of Physical Chemistry C, 2017, 116(39): 20839-20847.

[15] Fu S F, Zhu C Z, Du D, et al. Facile one-step synthesis of three-dimensional Pd-Ag bimetallic alloy networks and their electrocatalytic activity toward ethanol oxidation[J]. ACS Applied Materials & Interfaces, 2015, 7(25): 13842-13848.

[16] Jin C C, Wan C C, Dong R L. High activity of Pd deposited on Ag/C for allyl alcohol oxidation[J]. Electrochimica Acta, 2018, 262: 319-325.

[17] Zhang H C, Shang Y Y, Zhao J, et al. Enhanced electrocatalytic activity of ethanol oxidation reaction on palladium-silver nanoparticles via removable surface ligands[J]. ACS Applied Materials & Interfaces, 2017, 9(19): 16635-16643.

[18] Jo Y G, Kim S M, Kim J W, et al. Composition-tuned porous Pd-Ag bimetallic dendrites for the enhancement of ethanol oxidation reactions[J]. Journal of Alloys and Compounds, 2016, 688: 447-453.

[19] Yi Q F, Niu F J, Song L H, et al. Electrochemical activity of novel titanium-supported porous binary Pd-Ru particles for ethanol oxidation in alkaline media[J]. Electroanalysis, 2011, 23(9): 2232-2240.

[20] Zhang K, Bin D, Yang B B, et al. Ru-assisted synthesis of Pd/Ru nanodendrites with high activity for ethanol electrooxidation[J]. Nanoscale, 2015, 7(29): 12445-12451.

[21] Rezaee S, Shahrokhian S, Amini M K. Nanocomposite with promoted electrocatalytic behavior based on bimetallic Pd-Ni nanoparticles, manganese dioxide, and reduced graphene oxide for efficient electrooxidation of ethanol[J]. Journal of Physical Chemistry C, 2018, 122 (18): 9783-9794.

[22] Guo F, Li Y J, Fan B A, et al. Carbon- and binder-free core-shell nanowire arrays for efficient ethanol electrooxidation in alkaline medium[J]. ACS Applied Materials & Interfaces, 2018, 10(5): 4705-4714.

[23] Mavrokefalos C K, Hasan M, Rohan J F, et al. Enhanced mass activity and stability of bimetallic Pd-Ni nanoparticles on boron-doped diamond for direct ethanol fuel cell applications[J]. ChemElectroChem, 2018, 5(3): 455-463.

[24] Yao C Z(**姚陈忠**), Ma H X(**马会宣**), Wei B H(**卫博慧**). Electrochemical preparation of nanostructural Pt-Ni and Pd-Ni films for ethanol electrooxidation[J]. Journal of Electrochemistry(**电化学**), 2012, 18(2): 162-168.

[25] Mavrokefalos C K, Hasan M, Khunsin W, et al. Electrochemically modified boron-doped diamond electrode with Pd and Pd-Sn nanoparticles for ethanol electrooxidation[J]. Electrochimica Acta, 2017, 243: 310-319.

[26] Li Y H, Wang Y J, Mao H M, et al. Synthesis of carbon supported Pd-Sn catalysts by ethylene glycol method for ethanol electrooxidation[J]. International Journal of Electrochemical Science, 2016, 11(8): 7011-7019.

[27] Bai Y Z, Xu P L, Chao S J, et al. A facile one-step preparation of a Pd-Co bimetallic hollow nanosphere electrocatalyst for ethanol oxidation[J]. Catalysis Science & Technology, 2013, 3(10): 2843-2848.

[28] Wang A L, He X J, Lu X F, et al. Palladium-cobalt nanotube arrays supported on carbon fiber cloth as high-performance flexible electrocatalysts for ethanol oxidation [J]. Angewandte Chemie International Edition, 2015, 54 (12): 3669-3673.

[29] Tsui L K, Zafferoni C, Lavacchi A, et al. Electrocatalytic activity and operational stability of electrodeposited Pd-Co films towards ethanol oxidation in alkaline electrolytes[J]. Journal of Power Sources, 2015, 293: 815-822.

[30] Zhang J Y, Feng A N, Bai J, et al. One-pot synthesis of hierarchical flower-like Pd-Cu alloy support on graphene towards ethanol oxidation[J]. Nanoscale Research Letters, 2017, 12(1): 521.

[31] Zhang Z H, Zhang C, Sun J, et al. Ultrafine nanoporous PdFe/Fe_3O_4 catalysts with doubly enhanced activities towards electro-oxidation of methanol and ethanol in alkaline media[J]. Journal of Materials Chemistry A, 2013, 1 (11): 3620-3628.

[32] Lee Y W, Kim M, Kim Y, et al. Synthesis and electrocatalytic activity of Au-Pd alloy nanodendrites for ethanol oxidation[J]. The Journal of Physical Chemistry C, 2010, 114(17): 7689-7693.

[33] Qiu X Y, Dai Y X, Tang Y W, et al. One-pot synthesis of gold-palladium@palladium core-shell nanoflowers as efficient electrocatalyst for ethanol electrooxidation[J]. Journal of Power Sources, 2015, 278: 430-435.

[34] Park Y, Lee Y W, Kang S W, et al. One-pot synthesis of Au@Pd core-shell nanocrystals with multiple high- and low-index facets and their high electrocatalytic performance[J]. Nanoscale, 2014, 6(16): 9798-9805.

[35] Geraldes A N, Silva D F D, Pino E S, et al. Ethanol electrooxidation in an alkaline medium using Pd/C, Au/C and PdAu/C electrocatalysts prepared by electron beam irradiation[J]. Electrochimica Acta, 2013, 111(6): 455-465.

[36] Qin Y H, Li Y F, Lv R L, et al. Pd-Au/C catalysts with different alloying degrees for ethanol oxidation in alkaline media[J]. Electrochimica Acta, 2014, 144: 50-55.

[37] Zhang L, Wang X, Li X C, et al. One-step synthesis of palladium-gold-silver ternary nanoparticles supported on reduced graphene oxide for the electrooxidation of methanol and ethanol[J]. Electrochimica Acta, 2015, 172: 42-51.

[38] Kim D Y, Kang S W, Choi K W, et al. Au@Pd nanostructures with tunable morphologies and sizes and their enhanced electrocatalytic activity[J]. CrystEngComm, 2013, 15(35): 7113-7120.

[39] Chen H M, Xing Z L, Zhu S Q, et al. Palladium modified gold nanoparticles as electrocatalysts for ethanol electrooxidation[J]. Journal of Power Sources, 2016, 321: 264-269.

[40] Hostetler M J, Wingate J E, Zhong C J, et al. Alkanethiolate gold cluster molecules with core diameters from 1.5 to 5.2 nm: core and monolayer properties as a function of core size[J]. Langmuir, 1998, 14(1): 17-30.

[41] Shao M H, Odell J, Humbert M, et al. Electrocatalysis on shape-controlled palladium nanocrystals: oxygen reduc-

tion reaction and formic acid oxidation[J]. The Journal of Physical Chemistry C, 2013, 117(8): 4172-4180.

[42] Shao M H, Peles A, Shoemaker K, et al. Enhanced oxygen reduction activity of platinum monolayer on gold nanoparticles[J]. The Journal of Physical Chemistry Letters, 2011, 2(2): 67-72.

[43] Palomar-Pardavé M, Garfias-García E, Romero-Romo M, et al. Influence of the substrate's surface structure on the mechanism and kinetics of the electrochemical UPD formation of a copper monolayer on gold[J]. Electrochimica Acta, 2011, 56(27): 10083-10092.

[44] Plowman B J, Compton R G. Inhibition of Cu underpotential deposition on Au nanoparticles: The role of the citrate capping agent and nanoparticle size[J]. ChemElectroChem, 2014, 1(6): 1009-1012.

[45] Shao M H, Peles A, Odell J. Enhanced oxygen reduction activity of platinum monolayer with a gold interlayer on palladium[J]. The Journal of Physical Chemistry C, 2014, 118(32): 18505-18509.

[46] Cheng F L, Dai X C, Wang H, et al. Synergistic effect of Pd-Au bimetallic surfaces in Au-covered Pd nanowires studied for ethanol oxidation[J]. Electrochimica Acta, 2010, 55(7): 2295-2298.

[47] Liu L C, Corma A. Metal catalysts for heterogeneous catalysis: From single atoms to nanoclusters and nanoparticles[J]. Chemical Reviews, 2018, 118(10): 4981-5079.

钯原子修饰的金纳米颗粒乙醇氧化电催化剂

陈慧梅[1,2,3],朱尚乾[2],黄加乐[3],邵敏华[2*]

(1. 浙江医药高等专科学校制药工程学院, 浙江 宁波 315100; 2. 香港科技大学化学与生物工程系, 香港 999077;
3. 厦门大学化学化工学院, 化学工程与生物工程系, 福建 厦门 361005)

摘要: 钯催化剂对碱性溶液的乙醇电催化氧化反应表现较好的催化活性. 本文通过简单的化学沉积法, 将钯原子成功修饰到金纳米颗粒表面, 制备的催化剂对乙醇电催化氧化反应表现出比钯更好的催化性能. 研究发现,钯原子不均匀地覆盖在金核表面,部分金原子暴露在外层. 制备的催化剂的峰电流密度是钯催化剂的 4.6 倍,起始电势低 100 mV. 该催化剂较好的催化性能可能归因于金核的电子效应和表面双功能电催化反应机制.

关键词: 乙醇氧化;核壳;电催化作用;燃料电池;表面原子